OFFICE OF NAVAL RESEARCH
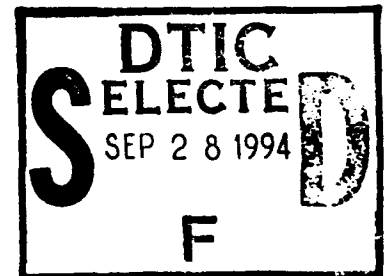
AD-A284 940

TECHNICAL REPORT NO. 13

ATOMIC SCALE FORCE MAPPING WITH
THE ATOMIC FORCE MICROSCOPE

by J.P. Cleveland, M. Radmacher and P.K. Hansma

Department of Physics

University of California, Santa Barbara

Santa Barbara, CA 93106

DTIC
SELECTED
SEP 2 8 1994
F

September 21, 1994

DTIC QUALITY INSPECTED 3

94-30898

The ability to recognize differences between atoms in topographically similar positions has been a long-standing goal in Atomic Force Microscopy, especially in a biological context. Mapping of forces (often attractive) at very small (< 5 A) tip-sample separations is one plausible way to achieve this. We have measured these types of forces above crystalline surfaces in water. Atomic resolution on attractive forces is demonstrated on the cleavage planes of calcite and muscovite mica. Atomic scale variations in the force between the tip and sample as a function of lateral position are observed on calcite.

Accesion For		
NTIS CRA&I	☑	
DTIC TAB	☐	
Unannounced	☐	
Justification		
By		
Distribution /		
Availability Codes		
Dist	Avail and / or Special	
A-1		

ATOMIC SCALE FORCE MAPPING WITH THE ATOMIC FORCE MICROSCOPE

J.P. CLEVELAND, M. RADMACHER, P.K. HANSMA
Physics Department
University of California, Santa Barbara
Santa Barbara, CA 93106
U.S.A.

ABSTRACT. The ability to recognize differences between atoms in topographically similar positions has been a long-standing goal in Atomic Force Microscopy, especially in a biological context. Mapping of forces (often attractive) at very small (<5 Å) tip-sample separations is one plausible way to achieve this. We have measured these types of forces above crystalline surfaces in water. Atomic resolution on attractive forces is demonstrated on the cleavage planes of calcite and muscovite mica. Atomic scale variations in the force between the tip and sample as a function of lateral position are observed on calcite.

1. Introduction

Recent work by Ohnesorge and Binnig[1] has shown that atomic resolution with the Atomic Force Microscope (AFM)[2,3] is possible at extremely small (<5 Å) tip-sample separations when the tip and sample are immersed in fluid.[4,5] Previous work in fluids at much larger length scales has shown that topography can be measured simultaneously with some material property (e.g. magnetism) by performing contact and then non-contact scans several 10's of nm above the surface.[6] The new work suggests that these ideas can be extended to atomic length scales and "atomic recognition" achieved. There have been several works suggesting that this is possible and investigating the nature and control of the expected non-contact forces.[7,8,9,10,11] All of these works predict that, given the current force resolution of the AFM and limitations on the cantilever stiffness imposed by mechanical instability in the presence of an attractive force gradient[12], this non-contact imaging will be possible only at small tip-sample separations like those used in reference 1. Here we have confirmed the work of reference 1 on the cleavage plane of calcite and extended their work to the cleavage plane of muscovite mica.

2. Materials and Methods

2.1 THE MICROSCOPE

All measurements were made using a standard Nanoscope II AFM[13] equipped with a glass fluid cell. A 0.78 μm-scanner with a 500 nm z-range was used for the mica work and a 15 μm-scanner with a 3.5 μm z-range was used for the calcite work. The Nanoscope controller was used to control lateral scanning and collect image data, but the z-piezo could be driven externally by a precision high-voltage power supply[14] floating on top of a

function generator[15]. This allowed us to generate AC voltages for the force scans while maintaining precise (sub-Ångstrøm) control of the DC offset.

For imaging, the function generator could be turned off and the power supply used to control the sample position. No feedback was used in collecting these images (the z-piezo was held at a fixed voltage throughout the image). Although this meant that sample tilt or drift in the z-direction were not corrected, it allowed precise control of tip-sample separation regardless of the sign of the force acting on the cantilever. The tilt also proved to be a useful tool for comparing contact and non-contact contrast in the same image. The fluid cell was always cleaned prior to the experiment by ultrasonication in a detergent[16] and then in Milli-Q[17] water (>18 MΩ). No O-rings were used.

Atomic resolution could usually be achieved immediately on both samples; however, both lateral and z-drift improved if the microscope was allowed to equilibrate for ~1 hr under a Neoprene insulating hood after filling the fluid-cell. Much of this initial drift is due to thermal bending of the cantilever itself[18,19].

2.2 SAMPLES AND CANTILEVERS

Muscovite mica was cleaved immersed in Milli-Q water and transferred to the fluid cell while still wet. Calcite ($CaCO_3$) was cleaved in air and immediately (< 5 min) transferred to the fluid cell. Calcite is slightly soluble in water, so the cell was given 30 minutes to come to chemical equilibrium (~50 μM). Calcite crystals in air were extremely hydrophilic after cleavage but slowly became hydrophobic over several hours, indicating some surface contamination or reconstruction happening on that time scale.

Single crystal silicon cantilevers with integrated oxide-sharpened tips were used as received[20]. We used the smallest, stiffest cantilever available. Scanning electron microscopy (SEM) showed the triangular cantilevers to be 82 μm long with 23 μm wide legs. The tips are sharp (20 nm end radius of curvature or less) with a high aspect ratio, especially near the end of the tip. The cost of sharpness is fragility. SEM of the tips after use at loads above 100 nN often showed the tip had fractured along a crystallographic plane during use. The cantilevers are known to have 1.8 to 2.0 nm of native oxide on the surface.[21]

The stiffness of the cantilevers was calibrated by pushing against a 1 cm cantilever constructed from 20 μm gold wire that had been previously calibrated by pushing against a microbalance. After calibrating one cantilever, the stiffness of other cantilevers of the same size could be estimated using the resonant frequency[22]. All cantilevers used here had a spring constant of 2.3 ± 0.1 nN/nm.

2.3 DATA PROCESSING

All of the images were flattened (the average of each scan line was subtracted). Although information about the DC deflection of the cantilever is lost over the entire image, it is still maintained within single scan lines. In addition to flattening, the mica atomic resolution image (Fig. 4B) was low pass filtered with a 1 Å cutoff.

The calcite force curves (Fig. 1) are raw data recorded in a bandwidth DC to ~25 kHz. To generate the mica force curve (Fig. 3), 32 sequential curves were aligned to compensate for drift and piezo hysteresis and then averaged. The AFM force data was then converted to a tip versus sample separation curve.[23] The algorithm for drift compensation also provided a value for the z-drift.
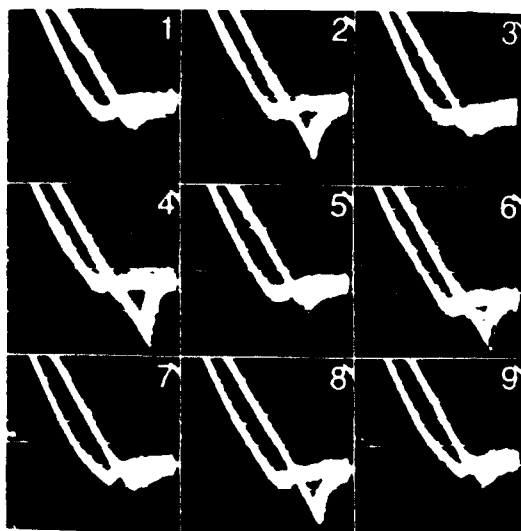
Fig.1 A series of atomic scale force curves on calcite in Milli-Q water. The X-axis is sample displacement, 4 Å per division; the Y-axis is cantilever deflection, 2 Å (460 pN) per division. The force curves were cycled at a frequency of 300 Hz and recorded on video, yielding about 10 force curves superimposed on each video frame. The lateral drift was calibrated at 0.7 Å/s by recording atomic resolution images with the slow scan axis disabled in two orthogonal directions. The force curves alternated between the two states shown in the odd and even frames with a period of 6-7 s (4.2 - 4.9 Å). Although there were small changes (<200 pN) in the approach curve, the dominate feature was the changing adhesion in the retract curve which alternated between ~ 1 nN and below our detection level. Even at a single lattice site several values of adhesion that may be quantized were possible (e.g. frame 6, 8). The displacement between the approach and retract curve is due the piezo and diminished appreciably at lower scan rates. Note that the approach and retract are sometimes hysteretic (adhesion is present in the retract) even though no mechanical instability is observed in the approach curve. This implies that the hysteresis might actually be due to some irreversible process in the force itself (e.g. bonding to the sample).

3. Results and Discussion

3.1 IMAGING FORCES AND SAMPLE DAMAGE

With the cantilevers used sample damage on mica occurred at loading forces near 10 nN. These damage pits could then be reproducibly imaged at lower forces and larger scan sizes. Usually the pit depths were integer multiples of 10 Å corresponding to the cleavage layers in mica. Careful control of force yielded pits with depths as small as 3 Å. These forces correlate well with some estimates of damage thresholds assuming atomic size contact areas published for other "hard" substrates.[24,25] Although "atomic-lattice" resolution could often be achieved even while damage was occurring, true atomic resolution could not.

3.2 CALCITE FORCE CURVES

Atomic scale force curves (Fig. 1) were recorded on the calcite cleavage plane. Lateral drifts of ~ 1 Å/s allowed us to sample the forces above many lateral positions on the crystal. Variations in the forces (mainly the adhesion) consistent with the lattice periodicity were observed. The data suggests that this adhesive force may be quantized even over individual lattice sites.[26]

3.3 CALCITE IMAGES

There has been much previous AFM work on the cleavage plane of calcite[27,28,29]. Fig. 2 shows two atomic resolution images taken about 15 minutes after the force curves shown in Fig. 1. Fig 2A was recorded while the sample drifted from non-contact towards contact. The image shows that the *lines* of upstanding oxygens on the cleavage plane can be detected from sever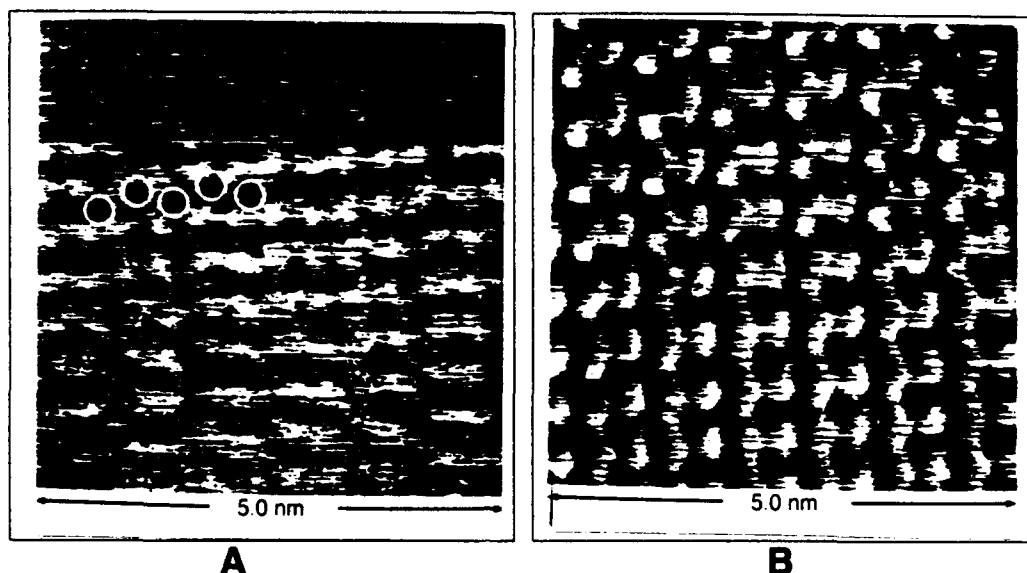al Ångstrøms away from the surface, but that the resolution required to resolve individual atoms can be achieved only in the last few Ångstrøms. The spacing of the lattice of dark spots (attractive points) is consistent with the model proposed in reference 1. Fig. 2B shows the type of variable contrast achieved on the repulsive force at higher loads. In general, the reciprocal lattice of these types of images remained the same, but the intensity of different spots varied drastically as a function of load[28] making it impossible to make assignments within the unit cell.

A   **B**

Fig. 2. Atomic scale images on calcite in Milli-Q water taken prior to the force measurements in Fig. 1. The 400 by 400 pixel images were acquired at a 78 Hz line rate (5.1 s per image). White corresponds to repulsive, and black to attractive deflections of the cantilever. The data shown is flattened (see text) but otherwise raw. (A) An image scanned from bottom to top while the tip drifted from non-contact (the bottom of the image) towards the surface (the top of the image) at less than 1 Å/s. At the bottom of the image, alternating lines of contrast are barely visible above the noise, but by the top of the image these lines are resolved to be the attractive 2-D lattice (white circles) associated with the upstanding oxygens in the carbonate groups (8.1 Å x 5 Å, 2 oxygens per unit cell). Imaging was interrupted, for an unknown reason, after about 75% of the image was acquired. (B) An image scanned from top to bottom taken in contact at a load of several nN. Once the tip was in contact with the sample, increasing the load resulted in a variety of contrasts. The reciprocal lattice of the images remained the same but drastic differences in spot intensities were observed for increasing load. Multiple tip contacts is a plausible explanation. Note that no assignments within the unit cell could be made under these higher load conditions.

3.4 MICA FORCE CURVES

Upon first engaging, an attractive force curve similar in shape to that in Fig. 3 but only about one-fifth (less than 1 Å of deflection) as strong was consistently observed. The attractive

Fig. 3. An averaged force vs tip-sample separation on mica in Milli-Q water. The zero on the x-axis has arbitrarily been set at the point where the sign of the force gradient changes. A sequence of 32 force curves cycled at 128 Hz was sampled by a computer with a data acquisition card at 400 points per cycle. The individual curves were aligned to compensate for drift and piezo hysteresis and then averaged. The non-contact noise in a bandwidth DC to ~25 kHz was 0.35 Å RMS before averaging and 0.06 Å RMS afterwards. The measured z-drift was 0.2 Å/s.
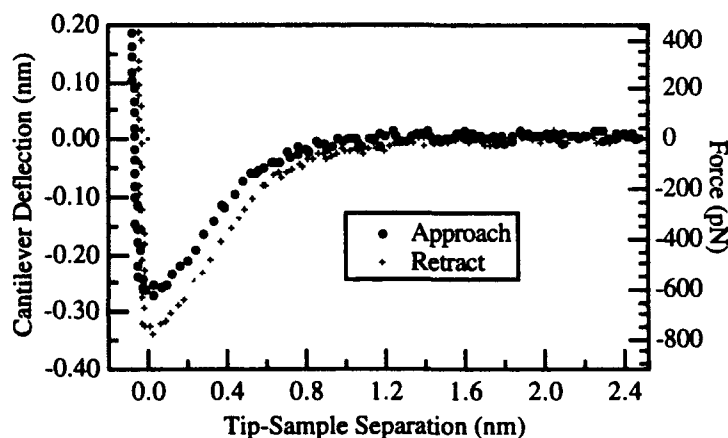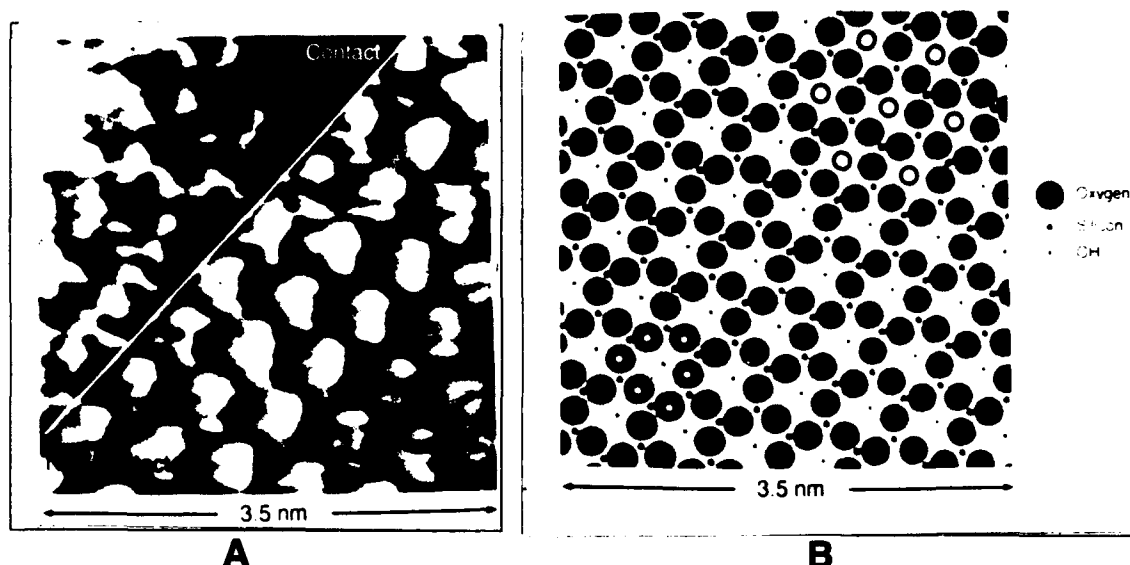
Fig. 4. Comparison of an atomic resolution image showing both contact and non-contact data with a model of the cleavage plane of muscovite mica. (A) Atomic resolution image of mica in Milli-Q water taken just prior to measuring Fig. 3. The 400 by 400 pixel image was acquired at a 78 Hz line rate. White corresponds to repulsive, and black to attractive deflections of the cantilever. The data were flattened (see text) and then low pass filtered with a 1 Å cutoff. The voltage to the z-piezo was held fixed during the entire image defining a flat plane in space. Because the sample was tilted slightly relative to this plane (1.9° in the fast scan direction and 1.3° in the slow scan direction), the tip moved towards and away from the sample 1.2 Å every fast scan line. The z-drift was 0.2 Å/s (see Fig. 3) so the sample also drifted 1 Å towards the tip over the entire image. If the drift is uniform, then in the right z-range there should be a "contact" and "non-contact" portion of the image separated by a straight line whose orientation is a function of both the drift rate and the sample tilt. The "contact" region should correspond to contrast generated on the portion of the force curve of Fig. 3 less than zero, and the "non-contact" region to contrast generated from separations greater than zero in Fig 3. The white line in the image marks what appears to be just such a line. The large lattice of white spots in the "non-contact" region is a lattice of areas where the cantilever was not deflected and therefore can probably be indexed to the lattice of "holes" (marked by the empty circles in Fig. 4B). Then, the dark rings surrounding these white spots (areas where the tip was attracted to the sample) could be indexed to the rings of oxygen atoms surrounding the "holes". As the model predicts, these rings are threefold symmetric around the "holes". Note that a slight attraction is barely resolved near the center of many of the white spots where an OH group is expected. (B) An atomic scale model of the cleavage plane of muscovite mica generated from crystallographic data[30] Assuming the potassium ions are in a diffuse double layer[31] and not bound well to the surface there are then three planes of atoms relevant to AFM imaging. The topmost layer is composed of rings of oxygen atoms (R = 1.4 Å) with threefold symmetry about the centers of the rings and a 5.2 Å center-to-center spacing. One such ring of oxygens is marked with white dots in the lower left-hand corner. The centers of these rings form the lattice of holes (open circles, upper right) normally imaged in AFM "atomic" resolution of mica. The next layer is located 0.6 Å beneath the oxygens and is composed of 75% Si (R= 0.42 Å) and 25% Al (R = 0.51 Å) randomly distributed. The final layer is OH groups located 2.3 Å beneath the oxygen rings. The OH groups are off-center of the oxygen rings because mica is monoclinic (ß = 95°). The OH groups have been made smaller than their true radius in the model to represent the fact that they are far beneath the cleavage plane.

forces were comparable to noise levels, making atomic resolution impossible. After increasing the force to the point where sample damage occurred and then decreasing the force again the force curve in Fig. 3 was observed on a new area of the sample. Clearly, some alteration of the tip occurred during the sample damage. The fracture angles observed in the SEM of the tips after use suggest that the tip cleaving is a likely explanation for the change in the force curve. Such a cleavage would expose an unoxidized surface and could still leave an atomically sharp tip behind.

3.5 MICA IMAGES

Fig. 4A shows an atomic resolution image achieved after the force curves of Fig. 3 were recorded demonstrating contact and non-contact atomic resolution. Even though the z-voltage was held constant throughout the entire image, sample tilt and drift allowed us to image at different tip-sample separations. Fig. 4B shows an atomic scale model of the cleavage plane in water.

4. Conclusion

The results presented here represent important steps towards an understanding of tip-sample interactions that will allow atomic recognition; however, there are still many hurdles to overcome. All the work here was done on atomically flat surfaces with no feedback, but the mapping of forces on "bumpy" surfaces such as biological samples will require the tracing of delicate contours with Ångstrøm precision. New types of feedback will need to be devised to control tip-sample separation precisely in cases where the forces are variable. There is also the problem of damage on samples much softer than those studied here. Because the mechanical instability puts a limit on cantilever stiffness, improvements must come in force detection techniques or active feedback techniques.

We and others have recently began mapping forces above the surface by rastering a volume using the piezo.[32,33,34] The work here is similar, but thermal drifts are utilized for scanning the sample slowly. If drift can be improved, active rastering of the sample in three dimension on the atomic scale will improve the data available.

Finally, it needs to be remarked that these types of results do not repeat easily. We found about 1 in 10 experiments behaved like those presented. The problem most likely lies in tip structure at the nanometer scale. There is obviously much room for improvement here. With the present levels of repeatability we at least have a framework to work within for understanding and improving these problems.

6. References

[1] F. Ohnesorge and G. Binnig, Science, **260**, 1451-1456 (1993)

[2] G. Binnig, C. F. Quate and C. Gerber, Phys. Rev. Lett., **56**, 930-933 (1986)

[3] D. Rugar and P. Hansma, Physics Today, **43**, 23-30 (1990)

[4] A. L. Weisenhorn, P. K. Hansma, T. R. Albrecht and C. F. Quate, Appl. Phys. Lett., **54**, 2651-2653 (1989)

[5] O. Marti, B. Drake and P. K. Hansma, Appl. Phys. Lett., **51**, 484 (1987)

[6] R. Giles, J. P. Cleveland, S. Manne, P. K. Hansma, B. Drake, P. Maivald, C. Boles, J. Gurley and V. Elings, Appl. Phys. Lett., **63**, 617-618 (1993)

[7] F. J. Giesibl, Phys. Rev. B, **45**, 13815-13818 (1992)

[8] C. Girard, D. Van Labeke and J. M. Vigoureux, Phys. Rev. B, **40**, 12133-12139 (1989)

[9] J. L. Hutter and J. Bechhoefer, J. Appl. Phys., **73**, 4123-4129 (1993)

[10] U. Hartmann, Phys. Rev. B, **43**, 2404-2407 (1991)

[11] J. E. Lennard-Jones and B. M. Dent, Trans. Faraday Soc., **24**, 92-108 (1928)

[12] D. Tabor and R. H. S. Winterton, Proc. Roy. Soc. A, **312**, 435-450 (1969)

[13] Digital Instruments, Santa Barbara, CA, USA

[14] Model 6116A, Hewlett-Packard, Santa Clara, CA, USA

[15] Model 184, Wavetec, San Diego, CA, USA

[16] RBS 35, Pierce, Rockford, IL, U.S.A.

[17] Millipore Systems, Burlington, MA, U.S.A.

[18] M. Radmacher, J. P. Cleveland and P. K. Hansma, Scanning, **submitted**, (1994)

[19] J. Mertz, O. Marti and J. Mlynek, Appl. Phys. Lett., **62**, 2344-2346 (1993)

[20] Park Scientific Inst., Sunnyvale, CA, USA

[21] Personal communication, Marco Tortonese, Park Scientific Inst., Sunnyvale, CA, U.S.A.

[22] J. P. Cleveland, S. Manne, D. Bocek and P. K. Hansma, Rev. Sci. Instr., **64**, 403-405 (1993)

[23] N. A. Burnham, R. J. Colton and H. M. Pollock, Nanotech., **4**, 64-80 (1993)

[24] W. Zhong, G. Overney and D. Tomanek, Europhys. Lett., **15**, 49-54 (1991)

[25] F. O. Goodman and N. Garcia, Phys. Rev. B (Condensed Matter), **43**, 4728-4731 (1991)

[26] J. H. Hoh, J. P. Cleveland, C. B. Prater, J.-P. Revel and P. K. Hansma, J. Am. Chem. Soc., **114**, 4917-4918 (1992)

[27] P. E. Hillner, S. Manne, P. K. Hansma and A. J. Gratz, Faraday Disc., **95**, 191-197 (1993)

[28] A. L. Rachlin, G. S. Henderson and M. C. Goh, Am. Mineralogist, **77**, 904-910 (1992)

[29] P. M. Dove and M.F. Jr. Hochella, Geochimica et Cosmochimica, **57**, 705-714 (1993)

[30] R.W.G. Wyckoff, *Crystal Structures* (Wiley, New York, 1964)

[31] J. N. Israelachvili, *Intermolecular and surface forces* (Academic Press, New York, 1992)

[32] M. Radmacher, J. P. Cleveland, M. Fritz, H. G. Hansma and P. K. Hansma, Biophys. J., **in press**, (1994)

[33] H. A. Mizes, K.-G. Loh, R. J. D. Miller, S. K. Ahuja and E. F. Grabowski, Appl. Phys. Lett., **59**, 2901-2903 (1991)

[34] D. R. Baselt and J. D. Baldeschwieler, in preparation (1994)